ORIGINAL ARTICLE

An Eight-Week *In Vivo* Study on the Clinical Signs of Systemic Toxicity and Bone Regenerative Performance of Composites Containing Beta Tricalcium Phosphate, Hydrogel and Melatonin in Adult New Zealand Rabbit (*Oryctolagus cuniculus*)

Mohamed Abdelrasoul[1], Jahangir Bin Kamaldin[2], Jer Ping Ooi[2], Ahmed Abd El-Fattah[1,3], Gihan Kotry[4], Omneya Ramadan[5], Sherif Kandil[1]

[1] Department of Material Science, Institute of Graduate Studies and Research, Alexandria University, El-Shatby, Alexandria 21526, Egypt
[2] Integrative Medicine Cluster, Advanced Medical and Dental Institute, Universiti Sains Malaysia, Bertam, 13200 Kepala Batas, Pulau Pinang, Malaysia
[3] Department of Chemistry, College of Science, University of Bahrain, Sakhir PO Box 32038, Kingdom of Bahrain
[4] Department of Oral Medicine and Periodontology, Faculty of Dentistry, Alexandria University, El-Shatby, Alexandria 21526, Egypt
[5] Department of Oral Pathology, Faculty of Dentistry, Alexandria University, El-Shatby, Alexandria 21526, Egypt

ABSTRACT

Introduction: Melatonin (MEL) loaded alginate-chitosan/beta-tricalcium phosphate (Alg-CH/β-TCP) composite hydrogel has been formulated as a scaffold for bone regeneration. MEL in the scaffold was anticipated to accelerate bone regeneration. The objective of this study is to observe signs of systemic toxicity and physical changes on surface defected bone for bone regenerative performance of the composite. **Methods:** The proximal-medial metaphyseal cortex of the left tibia of New Zealand white rabbit was the surgical site of the defect. A total of nine rabbits were randomly allocated to three groups; Group I; implanted with MEL loaded Alg-CH/β-TCP, Group II; Alg-CH/β-TCP and Group III defects were sham control. The rabbits were daily observed to determine systemic toxicity effects by composites. The physical changes to implanted site were observed using digital x-ray radiography and computerized tomography at weeks 0, 2, 4, 6 and 8 of post-implantation. **Results:** There were no clinical signs of systemic toxicity for all groups of rabbits. Digital radiography did not show adverse effects to the bone. Computerized tomography showed reduction in the area size and depth volume of the implantation site, but accelerated regeneration within the 8 weeks was not significantly different ($P<0.05$) between the groups. **Conclusion:** Overall, the study suggests that Alg-CH/β-TCP composite scaffolds with and without the addition of MEL are compatible to bone. The composite scaffolds reduced the area size and depth volume of the implanted site within the 8-week duration. However, no remarkable difference in the accelerated reduction of area size and depth volume was observed.

Keywords: Hydrogels, Beta-tricalcium phosphate, Melatonin, Bone regeneration, Tomography

Corresponding Author:
Mohamed Abdelrasoul, MSc
Email: mo_roshdy@yahoo.com
Tel: +20 100 350 8225

INTRODUCTION

Bone grafting has been introduced in surgery to support and enhance bone recovery from injury with materials from the patient's own body, synthetic, artificial, or natural sources. The material for bone grafting is expected to show characteristics of osteogenesis (bone re-regeneration), flexibility, biocompatibility, biodegradability, and sufficient mechanical strength to withstand soft tissue compressive forces during bone regeneration (1, 2). Nevertheless, some of the materials have shown downsides; including resorption of bone, negative immune responses, disease communication, limited biodegradability and inadaptability (1, 3).

A variety of synthetic bone grafts have been utilized to fill osseous defects following removal of bone tumors. Calcium phosphate ceramics are synthetic scaffolds that have been employed in orthopedics since the 1980s. Beta-tricalcium phosphate (β-TCP), which possesses a stoichiometry similar to the amorphous biologic precursors to bone minerals, shows a Ca-to-P molar ratio of 1.5 (4). Studies have demonstrated that β-TCP is biocompatible, bioactive, and osteoconductive. However, β-TCP has poor standalone flexibility, fatigue strength and is brittle in nature, and therefore, is not reliable as load bearing bone graft substitute (5, 6).

Biodegradable hydrogels are 3-D networks formed from hydrophilic polymers which are crosslinked to form insoluble polymer matrices. They are of particular significance because drugs, cells, and proteins, can be loaded into polymer solutions before administration. In addition, their aqueous environment allows transportation of substances such as nutrients and by-products from cell metabolism (7).

Alginate (Alg) and chitosan (CH) are natural polysaccharides that have been utilized to prepare hydrogels, due to their ability to form gels under well-defined conditions. They possess unique properties, including biodegradability, biocompatibility, non-antigenicity, and flexibility in hydrated environments. It has been reported that blending them appears to improve their mechanical properties and cell interactions (8, 9).

For this reason, it is desirable to develop a composite hydrogel with the favorable properties of both Alg-CH and β-TCP to produce a synthetic bone graft substitute. The designed composites are likely to display enhanced toughness and plasticity from the polymeric phase, as well as bioactivity and mineralization properties typical of the bioceramics (10).

Melatonin (MEL) is a hormone produced majorly by the pineal gland in the brain. MEL contributes to several physiological functions such as regulation of circadian rhythms, immunomodulation, and reproduction. Recently, the investigations of melatonin's local application potential benefits presented very promising results with bone related disorders. In vitro and in vivo studies have shown MEL to hold a positive accelerative effect on osteoblastic differentiation and bone healing, as well as inhibits osteoclast formation and osteoclastic activity via its free radical scavenging and anti-inflammatory actions (11, 12). Several animal studies have documented its biomimetic effect around dental implants (13, 14).

The objective of this study is to prepare a MEL loaded Alg-CH/β-TCP composite hydrogel as a bone grafting material and to study its effect on the acceleration of bone regenerative performance upon implantation in live animals. In addition, the in vivo clinical signs of systemic toxicity for the biocompatibility of the prepared materials were also observed.

MATERIALS AND METHODS

Materials

Low viscosity alginate powder was obtained from Sigma Aldrich Chemical Co., Germany. Chitosan, 93% deacetylation, and anhydrous calcium chloride were obtained from Oxford Co., India. Beta-tricalcium phosphate powder of size 50 nm was purchased from Nanostreams Co., UK. Melatonin 99+% with molecular weight of 232.28 was obtained from Alfa Aesar GmbH & Co KG, Germany. Anhydrous calcium chloride, Ammonia, ethanol, glacial acetic acid, and phosphate-buffered saline (PBS, pH 7.4) were purchased from Sigma Aldrich Chemical Co., Germany.

Synthesis and characterization of the Alg-CH/β-TCP composite scaffolds

Alg-CH/β-TCP composite scaffold was synthesized according to Venkatesan et al. (8). For the synthesis of Alg-CH/β-TCP composite hydrogel, first the β-TCP particles (0.2 g) were added to the Alg solution (3% w/v) in deionized water (100 mL) and stirred for 1 hour to make a homogenous solution. The pH of the prepared Alg/β-TCP solution was adjusted to 10 by adding drops of ammonia solution (25 %). Second, CH solution (1% w/v) was dissolved in acetic acid (2%, 50 mL), and was added into the Alg/β-TCP solution drop by drop under continuous stirring for 2 hours till a gel was formed. The gel solution was transported into a 96 well microplate (6.94 mm well diameter x 11.65 mm well height) and frozen at -24° C for one day and freeze dried to form scaffolds. The scaffolds were cross-linked by immersion in calcium chloride solution (10%, 100 mL) for 30 minutes, followed by soaking in absolute ethanol for 10 minutes. Finally, scaffolds were washed with an excess amount of deionized water, and freeze dried again for experimentation. For the loading of MEL into the Alg-CH/β-TCP composite scaffold, the MEL powder (0.2 g) was added to the CH solution, homogenized with vortex for 10 minutes before mixing with Alg/β-TCP solution, and the rest of the procedure was followed as described for the Alg-CH/β-TCP.

Scanning electron microscopy (SEM)

The morphology of the Alg-CH/β-TCP composite scaffold was examined using scanning electron microscopy (SEM) (JEOL 5300-JSM, Japan) operated between 15 and 30 keV. The samples were frozen under liquid nitrogen, mounted, and sputter-coated with gold to a thickness of 400 Å in a sputter-coating unit (JFC 1100 E) prior to imaging by SEM.

Swelling ratio

Alg-CH/β-TCP composite scaffold samples of different weights ranges between 0.4 g and 1.1 g were incubated in phosphate-buffered saline (PBS, pH = 7.4) at 37° C for two weeks to determine their water uptake. Samples were removed at the predetermined time periods and the excess water on the surface was wiped out using a tissue paper and then the samples were weighed. The swelling ratio of the scaffolds was determined using the following equation (15, 16):

$$DS\ (\%) = \frac{(W_w - W_d)}{W_d} \times 100$$

Where DS is the degree of swelling, while W_d and W_w are the dry and wet weights of the samples, respectively. Swelling ratios are expressed as a mean ± SD (n = 5).

Porosity

The porosity of the Alg-CH/β-TCP composite scaffolds was determined at 37° C by the liquid displacement method (17). Cylindrical scaffolds of different weight between 0.4 g and 1.1 g were immersed individually in a graduated cylinder containing deionized water (25 mL) for 24 h to achieve the equilibrium. Then the hydrogel scaffolds were freeze dried and the final weight recorded. The porosity of the scaffolds was calculated according to following equation (17, 18):

$$\text{Porosity (\%)} = \frac{(W_2 - W_1)}{\rho V_s} \times 100$$

Where W_1 and W_2 represent the weight of the hydrogel scaffolds before and after immersion in the distilled water, ρ is the density of water and V_s is the volume of the dried hydrogel scaffold. Porosity value was expressed as mean ± SD (n = 5).

Mechanical properties

The compressive stress and strain of the scaffold samples were measured using a mechanical testing machine (DMA 7e - Perkin Elmer). In this test the hydrogel samples were shaped as cylinders without lyophilization. The samples used were (1.5 cm diameter x 1 cm height) in dimension. Each hydrogel was tested until it fractured. The samples were investigated and the data was measured as a mean ± SD (n = 5).

The rabbit tibia bone defect model

Nine healthy female New Zealand white rabbits (*Oryctolagus cuniculus*) that were non-pregnant, aged between 10 and 12 months, approximately weighing 4 kg to 5 kg at the commencement of testing, were utilized in the study, that was approved by the Universiti of Sains Malaysia Institutional Animal Care and Use Committee (USM IACUC), number: USM/IACUC/2019/(117)(985).

The rabbits were housed in separate cages, permitted *ad libitum* admittance to conventional grain pellets and an unlimited supply of drinking water and subjected to 12 hour alternating light and dark cycles per day. The rabbits were acclimated for 14 days prior to implantation to ensure their health and stability.

The nine rabbits were randomly divided and allocated to one of the three groups (n = 3 per group); Group I, the defected left tibiae was implanted with the MEL loaded Alg-CH/β-TCP composite scaffold; Group II, the defected left tibiae was implanted with the Alg-CH/β-TCP composite scaffold without the addition of MEL and; Group III, the defected left tibiae of the rabbit was left untreated as a sham control.

Surgical and implantation procedure

Anesthesia was established by intramuscularly injecting the rabbits with a mixture of xylazine/ketamine (5 mg/kg and 35 mg/kg body weight respectively) after that, a mask was attached to the anesthetic gas device (1 - 3% isoflurane with 400-800 mL/min oxygen) then placed at the rabbit's nose. The rabbits were sustained under anesthesia and operated on a pre-warmed operating table. The rabbits' heart rate, peripheral oxygen saturation were measured and documented through a pulse oximeter. Once the effect was confirmed by means of no reflex upon pinching of the foot, the rabbit's tongue was pulled out to avoid suffocation and a local anesthetic, mepivacaine hydrochloride 2% with levonordefrin 1:20,000 injection was injected around the site of incision.

Bone defects (6 mm in length, 3 mm in width and 2 mm in depth) of approximately area size of 18 mm^2 with depth volume of 36 mm^3, spanning the metaphyseal region in the proximal-medial cortex of the left tibia of rabbits were created using a micro motor drill with a 2 mm surgical burr. All bone defects were drilled at distance of 16.88 ±3.13 mm from the medial condyle of the left tibia.

The periosteum end and skin were sutured with resorbable interrupted sutures. Observation were made to make sure hemostasis is achieved. The rabbits were placed back in their individual cages. Postoperative care of the rabbits comprised of intramuscular administration of an antibiotic, an anti-inflammatory medication and a pain reliever, respectively after 24 hours of the surgery; where enrofloxacin (5 mg/kg body weight) once daily for seven days, meloxicam (0.2 mg/kg body weight) and tramadol (2 mg/kg body weight) once daily for three days were injected, respectively (19).

Observation of clinical signs of systemic toxicity for the biocompatibility

The surgical sites were daily examined for local effects of clinical signs i.e. swelling, sepsis and leg deformation. Then the rabbit health in term of clinical signs of acute systemic toxicity i.e. severe pain, severe distress, moribund and mortality. Followed by behavioral observation, e.g. no mobility, inhibition of feeding/water intake and abnormality of gait. Then the physiological condition were examined by inspecting the regional lymph nodes and measuring the rectal temperature.

Observation of the physical changes on a surface defected bone for the performance

The physical changes on the surface of bone at the site of defect/implantation were observed using the digital x-ray radiography. The lateral digital radiographs model Phillips Digitaldiagnost by Phillips Medical Systems, Germany was used at 50 kV and 2.00 mAs, of the entire tibia of the three groups. Whereas for the physical changes on the area size, and depth volume of defect/implantation site, the computerized tomography model Discover NM/CT 670, by General Electric, China with x-ray tube of 120 kV and 205 mAs was used with 360° rotation and a nominal single collimation width

of 0.625 mm to capture the images. The measurement of physical change in term of area size and depth volume was computed by eliminating the uppermost and lowermost nearly 20% (1.250±0.625 mm) edges of the defects' computed tomographic slices, followed by 3D reconstruction of the defect shape allowing for the estimation of volume of the confined region of interest (ROI) of the defect/implantation site. The data sets were reconstructed and segmented for subsequent image processing using an OsiriX MD software version 5.8 (Bernex, Switzerland) to measure the surface area (mm^2) of the defect, as well as the volume (mm^3) of a ROI defect for all rabbits in the three groups.

The observations of digital x-ray radiography and computerized tomography were carried out post-defect/implantation at weeks 0, 2, 4, 6 and 8. The rabbits were anesthetized using a mixture of xylazine/ketamine (5 mg/kg and 35 mg/kg body weight respectively) intramuscularly before the imaging procedures.

Statistical analysis of the data

The observations on clinical signs of systematic toxicity were analyzed descriptively and the observation data of the area size and depth volume of defect/implantation site were analyzed inferentially using IBM SPSS software package version 20.0. For the inferential analysis, the Kolmogorov-Smirnov test was used to verify the normality of distribution of variables. ANOVA was used for comparing between groups. Significance of the obtained results was evaluated at the alpha 0.05 level.

RESULTS

Characterization of the Alg-CH/β-TCP composite scaffold

Figure 1a shows the SEM image and figure 1b shows the swelling ratio of the prepared Alg-CH/β-TCP composite scaffold. As shown in figure 1a, the SEM image exhibited the porous nature of the scaffold with pores that were spread over the entire structure. The calculated porosity value of the composite scaffold was about 83.64 ± 1.2%. Moreover, the SEM image revealed a uniform and homogeneous distribution of β-TCP particles throughout the composite hydrogel. No delamination was observed between the β-TCP particles and the polymer matrix demonstrating a close bonding between them which possibly will help to improve the mechanical properties. Figure 1b shows the swelling behavior of the composite hydrogel scaffold due to water uptake in distilled water at 37° C over two weeks. In general, the swelling ratio increased within the first day, and then decreased until the end of the test. More specifically, after one day, the swelling has induced a mass increase of 130 ± 5.2% and the final swelling after 2 weeks was 85± 3.8%.

The ultimate compressive strain, ultimate compressive strength, and Young's modulus of the Alg-CH/β-TCP composite scaffold were 26.4 ± 0.52%, 92.6 ± 6.3 MPa, and 144.3 ± 9.5 MPa respectively. Furthermore, all the composite scaffolds retained a flat sheet shape and did not spatter randomly by the end of the compression testing.

The clinical signs of systemic toxicity for the biocompatibility

The findings on the clinical signs observation are shown in Table I. Throughout the 8-week duration, all the rabbits of the three groups did not show any mortality or moribund, except for one of the rabbits in control group at week 6. The rabbit died at 6th week during the x-ray radiography session due to reaction with the xylazine-ketamine anesthetization. For all the groups, the rabbits did not show indications of severe distress, severe pain, inhibition of feeding/water intake and abnormality of gait. The surgical sites of the nine rabbits did not show any clinical signs of swelling, sepsis and leg deformation. The rectal temperature and lymph nodes size did not show any apparent change for all three groups.

Observation of the physical changes on a surface defected bone for the performance

The surface rendering images and gross examination of the tibia of each rabbit are shown in Figure 2. The images did not show any apparent injury to the bone such as fracture, deformation, dislocation or line of breakage on

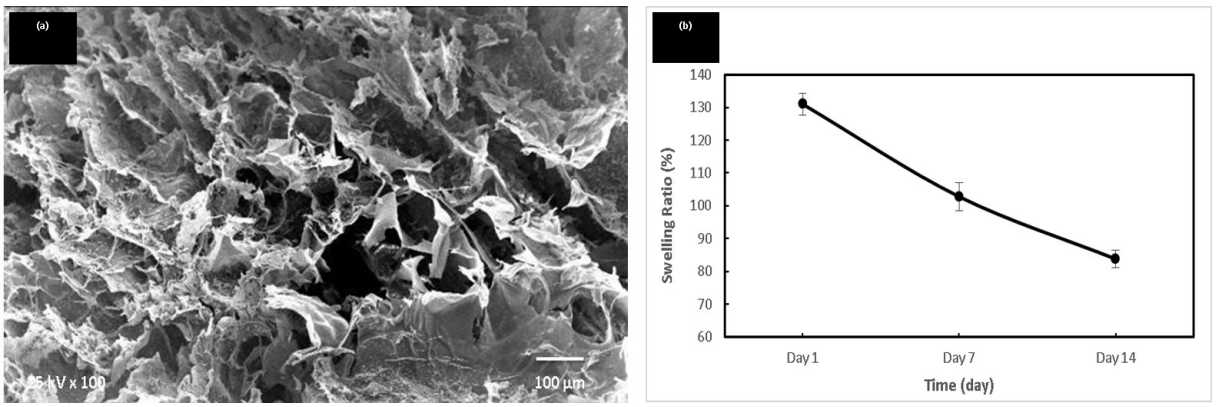

Figure 1: (a) Scanning electron microscope (SEM) image and (b) the swelling ratio of the prepared Alg-CH/β-TCP composite scaffold.

Table I: The clinical signs of acute, behavioral and physiological conditions of systemic toxicity of the New Zealand White rabbit (Oryctolagus cuniculus) been defected/ implanted with Alg-CH/β-TCP composites with and without melatonin on the left tibia for duration of 0-8 weeks

Group	Rabbit	Clinical Signs of Acute, Behavioural and Physical Conditions												
		PD	MD	MT	SL	SS	LD	FW	OS	TR	CS	NS	LN	RT
I	1	N	N	N	N	N	N	N	N	N	N	N	N	N
	2	N	N	N	N	N	N	N	N	N	N	N	N	N
	3	N	N	N	N	N	N	N	N	N	N	N	N	N
II	1	N	N	N	N	N	N	N	N	N	N	N	N	N
	2	N	N	N	N	N	N	N	N	N	N	N	N	N
	3	N	N	N	N	N	N	N	N	N	N	N	N	N
III	1	N	N	N	N	N	N	N	N	N	N	N	N	N
	2	N	N	N	N	N	N	N	N	N	N	N	N	N
	3	N	N	Y	N	N	N	N	N	N	N	N	N	N

*Note:
The acronyms for the clinical signs observation; yes observed (Y), none observed (N), severe pain/ severe distress (PD), moribund (MD), mortality (MT), swelling (SL), sepsis (SS), leg deformation (LD), inhibition of feeding/water intake (FW), over sleep (OS), tremors (TR), convulsions (CS), autonomic and central nervous systems disorder (NS), enlarged lymph nodes (LN), abnormal rectal temperature (RT).

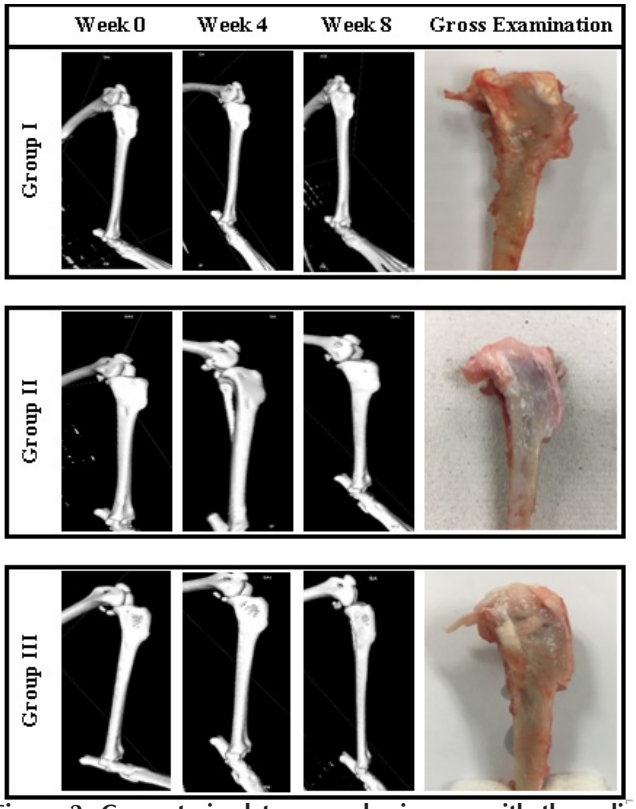

Figure 2: Computerized tomography images with three-dimensional surface rendering of defected/implanted site depth using the OsiriX software version 5.8 on the left tibia of the New Zealand White rabbit (*Oryctolagus cuniculus*) and gross examination of the control group and the treatment groups of Alg-CH/β-TCP composite scaffolds with and without MEL for duration of 0-8 weeks.

the bone, suggesting the surgery in making the defect and implantation with the bone graft composite did not cause any adverse effects to the bone structure in general.

The area size measurement of the defect/implantation site of each rabbit is exhibited in Figure 3 and Table II. In group I, the mean surface area of the defect site decreased from 23.1 ± 11.8 mm^2 at week 0 to 9.9 ± 2.9 mm^2 at week 4, and the final defect area size recorded on week 8 was 6.1 ± 0.6 mm^2. For group II, the mean surface area of the defect site decreased from 12.3 ± 2.5 mm^2 at week 0 to 9.5 ± 2.2 mm^2 at week 4, and the final mean defect area size recorded on week 8 was 7.4 ± 1.4 mm^2. On the other hand, the control group revealed a mean surface area of the defect site decrease

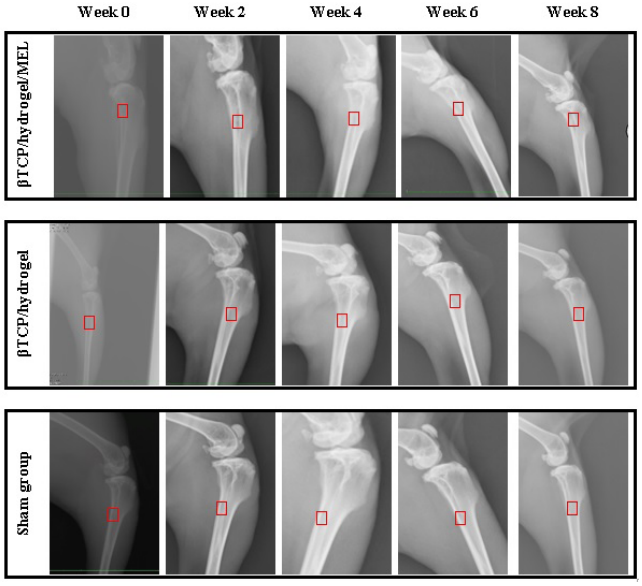

Figure 3: Digital radiography images of the defected/ implanted site on the left tibia of the New Zealand White rabbit (*Oryctolagus cuniculus*) of the control group and the treatment groups of Alg-CH/β-TCP composite scaffolds with and without MEL for duration of 0-8 weeks.

Table II: The area size of the defected/ implanted site of the control group and the treatment groups of Alg-CH/β-TCP composites with and without melatonin on the left tibia of the New Zealand White rabbit (Oryctolagus cuniculus) for duration of 0-8 weeks

	Surface areas (mm^2)				
Time	**Group 1[a]**	**Group 2[b]**	**Group 3[c]**	**F***	**P****
Week 0	23.1 ± 11.8	12.3 ± 2.5	13.8 ± 2.6	2.031	0.212
Week 2	13.7 ± 3.2	8.5 ± 1.5	12.2 ± 2.9	3.096	0.119
Week 4	9.9 ± 2.9	9.5 ± 2.2	11 ± 5	0.152	0.862
Week 6	6.4 ± 0.6	8.1 ± 1.1	5.9[#] ± 1.3	3.890	0.096
Week 8	6.1 ± 0.6	7.4 ± 1.4	5.1[#] ± 1.1	2.974	0.141

Note:
a Group 1: Hydrogel +Beta TCP + MEL
b Group 2: Hydrogel + Beta TCP
c Group 3: Sham group
#All groups (n = 3) except for week-6 and week-8 of group 3 (n = 2)
*F: F for ANOVA test
**P: value for comparing between the studied groups, statistical significant at P ≤ 0.05

from 13.8 ± 2.6 mm^2 at week 0 to 11 ± 5 mm^2 at week 4, and the final mean defect area size recorded on week 8 was 5.1 ± 1.1 mm^2. However, the ANOVA showed that reduction of size had no significance differences.

The computerized tomography imaging and depth volume of the defect/implantation site of each rabbit is displayed in Figure 4 and Table III, respectively, while the depth of the site rendered using the OsiriX software version 5.8 is shown in Figure 2. In group I, the mean volume of the defect site decreased from 4.19 ± 0.90 mm^3 at week 0 to 2.56 ± 0.47 mm^3 at week 4, and the final defect volume recorded on week 8 was 2.47 ± 0.47 mm^3. For group II, the mean volume of the defect site decreased from 3.20 ± 0.45 mm^3 at week 0 to 2.26 ± 0.36 mm3 at week 4, and the final mean defect volume recorded on week 8 was 1.42 ± 0.40 mm^3. On the other hand, the control group revealed a mean volume of the defect site decrease from 3.31 ± 0.81 mm^3 at week 0 to 1.96 ± 0.51 mm^3 at week 4, and the final mean defect volume recorded on week 8 was 1.14 ± 0.33 mm^3. However, the ANOVA showed that reduction of size had no significance differences.

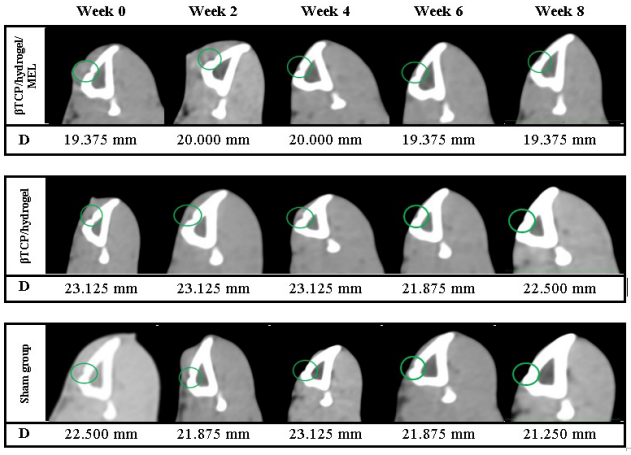

Figure 4: Computerized tomography images of defected/ implanted site depth using the OsiriX software version 5.8 on the left tibia of the New Zealand White rabbit (*Oryctolagus cuniculus*) of the control group and the treatment groups of Alg-CH/β-TCP composite scaffolds with and without MEL for duration of 0-8 weeks. D: Distance (in mm) from the head of the medial condyle of left tibia

Table III: The depth volume of the defected/ implanted site of the control group and the treatment groups of Alg-CH/β-TCP composites with and without melatonin on the left tibia of the New Zealand White rabbit (*Oryctolagus cuniculus*) using the computerized tomography image calculated using the OsiriX software version 5.8 for duration of 0-8 weeks

	Depth Volume (mm^3)				
Time	**Group 1[a]**	**Group 2[b]**	**Group 3[c]**	**F***	**P****
Day 1	4.2 ± 1.1	3.2 ± 0.5	3.3 ± 0.8	1.295	0.341
Week 2	3.7 ± 1.2	2.6 ± 0.1	3.2 ± 1.0	1.099	0.392
Week 4	2.6 ± 0.6	2.3 ± 0.4	2.0 ± 0.5	1.132	0.383
Week 6	2.1 ± 0.7	1.7 ± 0.4	2.1[#] ± 0.1	0.663	0.555
Week 8	2.5 ± 0.6	1.4 ± 0.4	1.1[#] ± 0.3	5.990	0.047

Note:
a Group 1: Hydrogel +Beta TCP + MEL
b Group 2: Hydrogel + Beta TCP
c Group 3: Sham group
#All groups (n = 3) except for week-6 and week-8 of group 3 (n = 2)
*F: F for ANOVA test
**P: value for comparing between the studied groups, statistical significant at P ≤ 0.05

DISCUSSION

The advances in the biomaterials field allowed better designing and processing of new materials in order to properly address cellular activity. This is an essential point to be tackled as the regeneration outcome depends merely on the cellular functions. These advances will result in more convenient options for the physicians and better treatment outcomes for the patients (20).

In this work, we have successfully prepared and characterized a composite hydrogel scaffold composed of Alg-CH/β-TCP and loaded with MEL. The SEM images showed well distribution of β-TCP particles within the polymer matrix and proved the porous nature of the scaffold with porosity over 80%. This porosity would allow cells to migrate into and populate the scaffold to facilitate vascularization and structural integration with the surrounding tissue. The water uptake ability of the scaffolds is measured by the swelling behavior of the scaffold in PBS solution. The composite scaffold is hydrophilic, thus the scaffold will enable the absorption of body fluid, which consists of water mainly, and is important for the diffusion of nutrients and metabolites. Moreover, the surface generally increases upon swelling of the scaffold, which is suitable for more cell adhesion and infiltration (21-23).

The mechanical properties of the scaffold are another critical feature that must be considered for bone tissue engineering applications. Scaffolds need good mechanical properties to maintain their shape during culturing and the surgical procedures of transplantation, and also to resist loading after implantation. It was worth mentioning that the incorporation of β-TCP particles as a reinforcing material in the scaffold increased the ultimate compressive strain, ultimate compressive strength, and Young's modulus. The improvement in mechanical properties of Alg-CH/β-TCP composite hydrogel could be attributed to the strong interfacial interaction between β-TCP and polymer phase gained from the formation of the hydrogen bond (24, 25).

The rabbit was the experimental animal model of choice due to the resemblance of bone mineral density of its mid-diaphyseal bone with that of human. Another reason was the ease of housing and handling this animal model. The timeframe of eight weeks was selected as the rabbits have a higher metabolism and bone turnover than humans, and at eight weeks healing was almost complete (26, 27).

Furthermore, the *in vivo* results of this study tested

the potential use of a digital radiography and human CT to evaluate the biomimetic effects of MEL loaded beta tricalcium phosphate composite scaffold and its capability to detect the differences with the regenerative potential of the polymeric hydrogel and beta tricalcium phosphate without melatonin. Ooi et al. (19) reported that human CT was a valuable tool in detection of changes in implantation sites of large size defects. Nevertheless, for smaller critical size defects as in this study the CT was not distinctive of the regenerative potential of the implantation material.

The human CT used was not sensitive enough to detect the regenerative potentials of the hydrogels compared to the control, as opposed to the enhanced scale of a micro CT where follow up and tracking of the implanted material is feasible, as well as the ability to determine the percentage and density of regenerated mineralized tissue.

CONCLUSION

Overall, the study suggests that both the Alg-CH/β-TCP composite scaffolds with and without the addition of MEL were receptive by the bone without adverse effects of systemic toxicity. Further the composite scaffolds have reduced the area size and depth volume of the defected/implanted site within the 8-week duration. However, there was no remarkable difference in the acceleration in reduction of the area size and depth volume among the groups. In order to elucidate the important role of MEL in the bone injury recovery a larger defect/implantation area or micro computerized tomography is required. Therefore, it is essential for the MEL loaded Alg-CH/β-TCP composite scaffolds to be evaluated in larger defect/implantation site e.g. femur head and calvarias or in a larger bone model, such as dog.

ACKNOWLEDGEMENTS

This work was possible through a research attachment at the Advanced Medical and Dental Institute, Universiti Sains Malaysia, Malaysia.

REFERENCES

1. Göransson A, Arvidsson A, Currie F, Franke-Stenport V, Kjellin P, Mustafa K, et al. An in vitro comparison of possibly bioactive titanium implant surfaces. J Biomed Mater Res – Part A. 2009;88:1037-1047.
2. Schulten EA, Prins HJ, Overman JR, Helder MN, Ten Bruggenkate CM, Klien-Nulend J. A novel approach revealing the effect of a collagenous membrane on osteoconduction in maxillary sinus floor elevation with β-tricalcium phosphate. Eur Cell Matter. 2013;25:215-238.
3. Dalby MJ, Riehle MO, Johnstone HJH, Affrossman S, Curtis ASG. Polymer-Demixed Nanotopography: Control of Fibroblast Spreading and Proliferation. Tissue Eng. 2003;8:1099-1108.
4. Seidenstuecker M, Ruehe J, Suedkamp NP, Serr A, Wittmer A, Bohner M, et al. Composite material consisting of microporous β-TCP ceramic and alginate for delayed release of antibiotics. Acta Biomaterialia. 2017;51:433-446.
5. Lee JH, Ryu MY, Baek HR, Lee HK, Seo JH, Lee KM, et al. The effects of recombinant human bone morphogenetic protein-2-loaded tricalcium phosphate microsphere-hydrogel composite on the osseointegration of dental implants in minipigs. Artif Organs. 2014;38(2):149-158.
6. Coelho PG, Freire JN, Granato R, Marin C, Bonfante EA, Gil JN, et al. Bone mineral apposition rates at early implantation times around differently prepared titanium surfaces: a study in beagle dogs. Int J Oral Maxillofac Implant. 2011;26:63-69.
7. Fedorovich NE, Alblas J, de Wijn JR, Hennink WE, AJ Verbout, WJA Dhert. Hydrogels as extracellular matrices for skeletal tissue engineering: state-of-the-art and novel application in organ printing. Tissue Engineering. 2007;13(8):1905-1925.
8. Venkatesan J, Bhatnagar I, Kim S. Chitosan-alginate biocomposite containing fucoidan for bone tissue engineering. Mar Drugs. 2014;12:300-316.
9. Aston R, Wimalaratne M, Brock A, Lawrie G, Grøndahl L. Interactions between chitosan and alginate dialdehyde biopolymers and their layer-by-layer assemblies. Biomacromolecules. 2015;16(6):1807-1817.
10. Kuttappan S, Mathew D, Nair MB. Biomimetic composite scaffolds containing bioceramics and collagen/gelatin for bone tissue engineering - A mini review. Int J Biol Macromol. 2016;93(Pt B):1390-1401.
11. Perez-Heredia M, Clavero-González J, Marchena-Rodríguez L. Use of melatonin in oral health and as dental premedication. J Biol Res (Thessalon). 2015;22:13.
12. Gómez-Moreno G, Aguilar-Salvatierra A, Boquete-Castro A, Guardia J, Piattelli A, Perrotti V, et al. Outcomes of topical applications of melatonin in implant dentistry: a systematic review. Implant Dent. 2015;24(1):25-30.
13. Cutando A, Gómez-Moreno G, Arana C, Muñoz F, Lopez-Peña M, Stephenson J, et al. Melatonin stimulates osteointegration of dental implants. J Pineal Res. 2008;45:174-179.
14. Calvo-Guirado JL, Ramírez-Fernández MP, Gómez-Moreno G, Maté-Sánchez JE, Delgado-Ruiz R, Guardia J, et al. Melatonin stimulates the growth of new bone around implants in the tibia of rabbits. J Pineal Res. 2010;49:356-363.
15. Devine DM, Higginbotham CL. Synthesis and characterisation of chemically crosslinked N-vinyl pyrrolidinone (NVP) based hydrogels. Eur Polym J. 2005;41:1272-1279.
16. Zhong X, Ji C, Chan AK, Kazarian SG, Ruys

A, Dehghani F. Fabrication of chitosan/poly(ε-caprolactone) composite hydrogels for tissue engineering applications. J Mater Sci Mater Med. 2011;22:279-288.
17. Peter M, Binulal NS, Soumya S, Nair SV, Furuike T, Tamura H,et al. Nanocomposite scaffolds of bioactive glass ceramic nanoparticles disseminated chitosan matrix for tissue engineering applications. Carbohydr Polym. 2010;79(2):284-289.
18. Sankar D, Chennazhi KP, Nair SV, Jayakumar R. Fabrication of chitin/poly(3-hydroxybutyrate-co-3-hydroxyvalerate) hydrogel scaffold. Carbohydr Polym. 2012;90(1): 725-729.
19. Ooi JP, Kasim SR, Shaari RB, Saidin NA. In vivo efficacy and toxicity of synthesized nano-β-tricalcium phosphate in a rabbit tibial defect model. Toxicol Res Appl. 2018;2:1-9.
20. Pina S, Oliveira JM, Reis RL. Natural-based nanocomposites for bone tissue engineering and regenerative medicine: a review. Adv Mater. 2015;27(7):1143–1169.
21. Roberts J J, Earnshaw A, Ferguson VL and Bryant SJ. Comparative study of the viscoelastic mechanical behavior of agarose and poly(ethylene glycol) hydrogels. J Biomed Mater Res B Appl Biomater. 2011;99:158-169.
22. Killion JA, Kehoe S, Geever LM, Devine DM, Sheehan E, Boyd D, et al. Hydrogel/bioactive glass composites for bone regeneration applications: synthesis and characterisation. Mater Sci Eng C Mater Biol Appl. 2013; 33: 4203-4212.
23. Sharma C, Dinda AK, Potdar PD, Chou CF, Mishra NC. Fabrication and characterization of novel nano-biocomposite scaffold of chitosan-gelatin-alginate-hydroxyapatite for bone tissue engineering. Mater Sci Eng C Mater Biol Appl. 2016;64:416-427.
24. Sarker A, Amirian J, Min YK, Lee BT. HAp granules encapsulated oxidized alginate-gelatin-biphasic calcium phosphate hydrogel for bone regeneration. Int J Biol Macromol. 2015;81:898-911.
25. Gantar A , Drnovšek N, Casuso P, Vicente AP, Rodriguez J, Dupin D, et al. Injectable and self-healing dynamic hydrogel containing bioactive glass nanoparticles as a potential biomaterial for bone regeneration. RSC Adv. 2016; 6:69156-69166.
26. Wang X, Marbrey JD, Agrawal CM. An interspecies comparison of bone fracture properties. Biomed Mater Eng. 1998;8(1):1–9.
27. Abedi G, Jahanshahi A, Fathi MH, Haghdost IS, Veshkini A. Study of nano-hydroxyapatite/zirconia stabilized with yttria in bone healing: histopathological study in rabbit model. Pol J Pathol. 2014;65(1):40-47.